Clays and Clay Minerals, Vol. 38, No. 4, 426–436, 1990.

DIAGENESIS OF OLIGOCENE-MIOCENE VITRIC TUFFS TO MONTMORILLONITE AND K-FELDSPAR DEPOSITS, DURANGO, MEXICO

LIBERTO DE PABLO-GALAN

Instituto de Geologia, Universidad Nacional Autonoma de Mexico
Ciudad Universitaria, 04510 Mexico, D.F., Mexico

Abstract—Montmorillonite and K-feldspar deposits of potential economic interest occur in the Late Oligocene-Miocene tuffs of the Vizcarra Formation in the state of Durango, Mexico. The two minerals were formed separately from rhyodacitic to rhyolitic pyroclastic deposits in a closed hydrologic system and diagenetically altered following two different patterns. In material deposited on dry land the glass was completely replaced by K-feldspar, and the interstices between the replaced glass bubbles and shards were filled with chalcedony, quartz, and albite. Pyroclastic material deposited in an alkaline lacustrine environment were diagenetically altered to montmorillonite, which formed the bentonitic tuffs widely exposed beneath the K-feldspar-rich tuff. These bentonitic tuffs contain as much as 85% montmorillonite plus authigenic chalcedony and quartz. Pyrogenic sanidine, quartz, and oxybiotite, coarse glass shards, and clastic grains make up about 8% of the clay-rich tuffs. The composition of the montmorillonite corresponds to the formula $(Si_{3.88}Al_{0.12})(Al_{1.41}Mg_{0.59})O_{10}(OH)_2(Ca_{0.07}Mg_{0.11}Na_{0.28}K_{0.06})$. The montmorillonite is dioctahedral, the surface acidity is of the Lewis type, and the clay swells to one- and two-layer complexes. The cation-exchange capacity is 64 meq/100 g; base exchange is Ca^{2+}, 15; Mg^{2+}, 20; Na^{+}, 4.1; and K^{+}, 1.0 meq/100 g. Its interlamellar charge is 18.6 microcoulombs/cm^2. Dacitic pyroclastics were deposited later at higher elevations along the margins of the basin. Percolating solutions apparently removed a siliceous leachate from the dacitic glass and partially altered it to clinoptilolite.

Key Words—Clinoptilolite, Diagenesis, Energy-dispersive X-ray spectroscopy, K-feldspar, Montmorillonite, Pyroclastic, Scanning electron microscopy, Tuff.

INTRODUCTION

Volcanism during the Late Oligocene-Miocene in Mexico produced extensive deposits of rhyodacitic and dacitic pyroclastics, which, in spite of their abundance and the presence of potentially economic deposits of non-metallic minerals that resulted from them (de Pablo-Galan, 1979), have scarcely been studied. This paper attempts to add to the knowledge of them and discusses the mineralogy, geochemistry, and petrology of bentonitic and K-enriched altered tuffs of the Vizcarra Formation and of the dacitic tuffs of the La Zorra Formation. Reactions involving the transformation of rhyodacitic glass to potentially economic montmorillonite and K-feldspar deposits are emphasized, along with the reactions of the dacitic glass to clinoptilolite.

GEOGRAPHIC AND GEOLOGIC SETTING

The tuffs discussed herein are part of the Upper Tertiary volcanic series that covers the Mesa Central, in the state of Durango, which is elongated NW-SE and is characterized by plutonic and hypabyssal intrusions and volcanic rocks that overlie the Mesozoic sediments (de Cserna-Gombos, 1956; Enciso, 1968; Carrasco, 1980). The volcanic rocks are exposed in the Cuencame-Lagunilla area at 103°25′–104°20′ W longitude and 24°50′–25°00′ N latitude and are part of a larger area mapped by Enciso (1968) in his Hoja Cuencame. The area is shown on the geologic maps (1:50,000) of Lagunilla and Cuencame (Direccion de Estudios del Territorio Nacional, 1978a, 1978b). These tuffs also crop out in the area between 103°40′–104°20′ W longitude and 25°00′–25°15′ N latitude, shown on the 1:50,000 maps of Rodeo, Velardena, and Nazas (Direccion de Estudios del Territorio Nacional, 1978c, 1978d, 1978e).

The geology of the area, based on the work of Enciso (1968), Direccion de Estudios del Territorio Nacional (1978a, 1978b, 1978c, 1978d, 1978e), and Lopez-Ramos (1983), is shown in Figure 1. The mountainous area around the valley of Lagunilla-Cuencame-Pedricena is underlain by Cretaceous limestones of the Cuesta del Cura, Aurora, and La Pena Formations, which underlie the clayey and gypsiferous limestones of the Indidura Formation (Razo, 1960; Enciso, 1968; Roldan, 1969). The Lower Tertiary is represented by the Ahuichila Formation, which consists of conglomerate and calcareous breccia. The Oligocene-Miocene rocks are andesite, rhyolite, basalt, and their tuffs, all well exposed throughout the area. Also present are the tuffs of the Vizcarra Formation, which are characterized by their white and pink colors and by their low topographic relief, generally <100 m at elevations of 1128 m above sea level (Figure 2). The darker colored dacitic tuffs of the La Zorra Formation (Enciso, 1968) are about 300 m thick and crop out at elevations >1420 m. The Vizcarra Formation resembles the Santa Barbara Formation exposed southeast of Durango (Cordoba, 1960) and the San Pablo Formation described by Roldan (1969) southeast of Cuencame. Field observations suggest that pyroclastic material transported as a "nueé ardente" was deposited in the basin, over the Cretaceous sediments. Subsequent diagenetic alteration of the material deposited on high dry ground formed the K-rich tuff now represented in the upper part of the Vizcarra Formation, whereas the material deposited in the lacustrine environment altered to the green and pink smectites, which now crop out at elevations of 1340 m in the Cuencame-Lagunilla valley and extend around Pedricena and to the west towards Rodeo and Nazas where they are exposed at eleva-

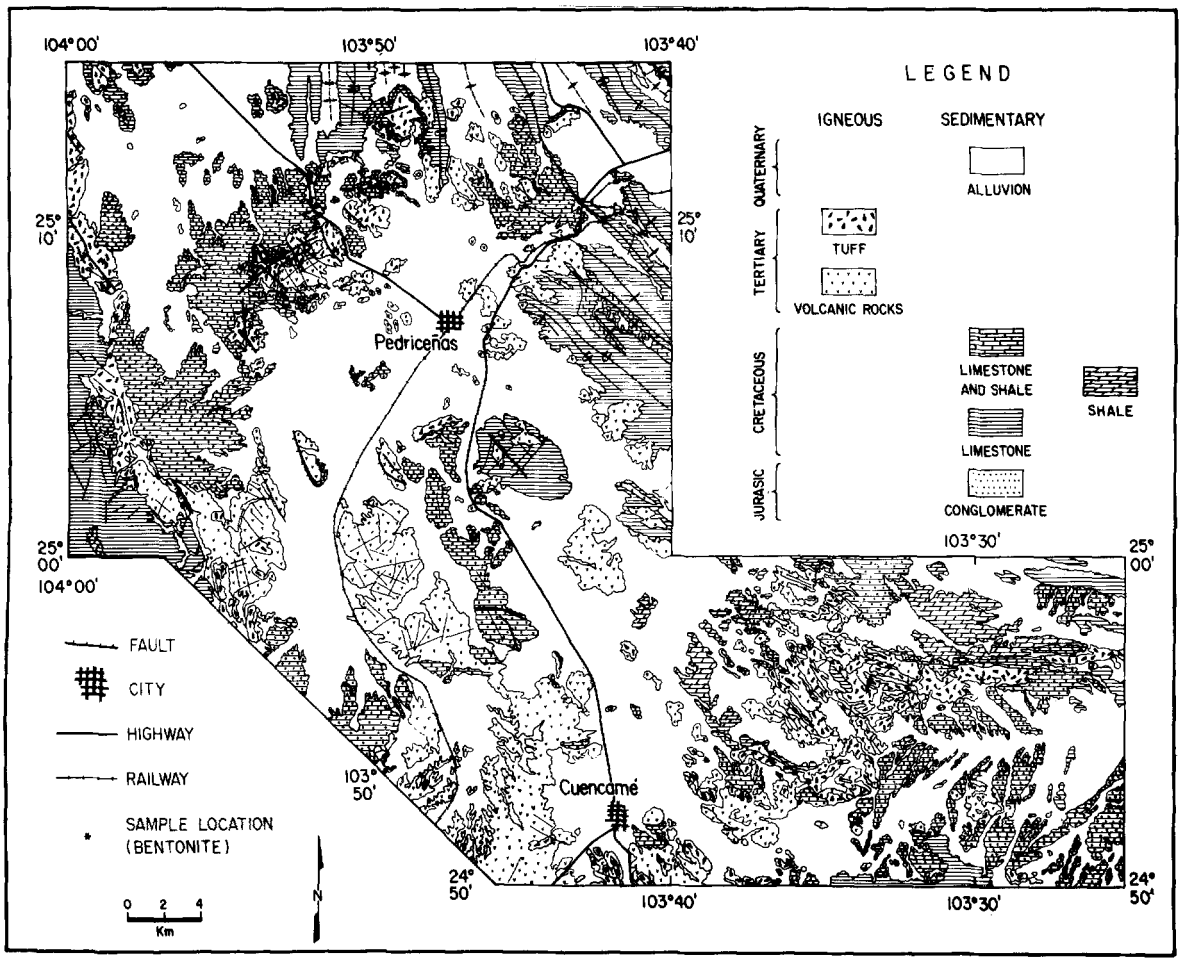

Figure 1. Map of area between 103°25′–104°00′ W longitude and 24°50′–25°15′ N latitude, in state of Durango, Mexico. Data taken from Enciso (1968), Direccion de Estudios del Territorio Nacional (1978a, 1978b, 1978c, 1978d, 1978e), and Lopez-Ramos (1983). Main deposits of smectite are located east of Cuencame and west of Pedricena.

tions of 1128 m (Figure 2). Therefore, an extensive area having a thick deposit of smectite of potential economic interest is indicated.

The dominant lithology of the area is the Late Oligocene-Miocene altered vitric tuff which crops out in the eastern and northwestern part of the basin as a white and pink rock, 2–6 m thick. This tuff is fine-grained and contains altered glass bubbles and shards and minor phenocrysts of feldspar, quartz, and biotite, with local secondary calcite and gypsum. A silicified tuff locally crops out on top. The altered vitric tuff is underlain by bentonitic tuff at elevations of 1134 m above sea level near Pedricena and of 1344 m east of Cuencame (Figure 2). The two tuffs comprise the Vizcarra Formation (Enciso, 1968). The bentonite in contact with the overlying altered tuff is green, <50-cm thick, and changes sharply to pink bentonite, which is generally exposed 4–8 m above a concealed lower contact. The bentonites have a similar mineralogy, which includes essential smectite and minor feldspar and quartz phenocrysts, glass shards, and clastic grains.

A unit of dacitic vitric tuff containing local basalt flows is exposed at elevations of 1420 m on the southern and western margins of the depositional basin (Figures 1 and 2) and is referred to as the La Zorra Formation (Enciso, 1968). It is dark colored and contains glass, pyrogenic plagioclase and quartz, and authigenic zeolite.

SAMPLING AND ANALYTICAL METHODS

The tuffs were sampled at the localities of Mesa de Los Difuntos, northwest of Pedricena; Cerro Prieto, east of Nazas; and San Antonio de Ojo Seco and Las Cuevas, east of Cuencame (Figure 1). About 100 samples were collected, but only those which are most representative are included in this paper.

Optical microscopy, utilizing thin sections and oil-immersion methods, and X-ray powder diffraction (XRD), using filtered CuKα radiation, were used to identify the various minerals and their interrelationships. Scanning electron microscopy (SEM) coupled to energy-dispersive X-ray spectrometry (EDX) was used to study the microtextural relations, morphology, and composition of minerals. The authigenic feldspar filling the altered glass bubbles was so finely crystalline that

detailed measurements of the optic angle to differentiate between sanidine and orthoclase were not possible; hence, its identification as K-feldspar had to rely on the chemical composition determined by EDX. Plagioclase of a composition near the albite end member was similarly characterized. Chalcedony was seen optically as a low-birefringent, massive phase, filling interstices between the altered glass shards, and was locally altered to saccharoidal quartz; cristobalite was identified by XRD. Chemical analyses by EDX were somewhat difficult due to the nature of the clays and the non-planar surface of the specimens.

The chemical composition of the tuffs was analyzed by X-ray fluorescence (XRF) spectrometry and by wet-chemistry procedures for Na, Cl, SO_4, CO_2, and H_2O; total Fe is reported as Fe_2O_3. The Bouyoucos hydrometer was used to determine the particle-size distribution. The cation-exchange capacity and exchangeable cations were analyzed by the usual techniques (Jaynes and Bigham, 1986). The smectite, separated after sedimenting the coarse components, was K-saturated and used to establish the nature of the interlamellar charge, recording the displacement of the 001 reflection before and after heating to 300°C (Weaver, 1958; Schultz, 1969). The site of the charge was located on Li-smectite by the position of the 001 plane before and after heating to 225° and glycolating (Greene-Kelley, 1955; Schultz, 1969). The swelling behavior was followed on Na-smectite saturated with Li for as long as 115 hr (Low, 1981; Sposito *et al.,* 1983). Na-smectite, saturated with pyridine and heated at 150° and 400°C, allowed recognition of the surface acidity of the clay according to the displacement of the infrared absorption bands in the 1430–1600-cm^{-1} region (Perry, 1983; Svoboda and Kunze, 1966; Ward, 1968; Wright *et al.,* 1972; Occelli and Tindwa, 1983). For the IR analysis, the treated smectite was mixed with dry KBr and pressed to thin wafers, which were analyzed in a single-beam Perkin-Elmer 783 Spectrometer at wavelengths from 4000 to 200 cm^{-1}.

RESULTS

The authigenic minerals identified in the altered vitric tuff are K-feldspar, chalcedony, cristobalite, quartz, and albite. K-feldspar and albite were differentiated by SEM and EDX as Si-, Al-, K-, and Na-containing phases. In the bentonitic tuff, montmorillonite and cristobalite are the two main authigenic minerals.

The authigenic minerals in the dacitic vitric tuff are a noncrystalline aluminosilicate phase, clinoptilolite, cristobalite, and halite. The noncrystalline aluminosilicate phase was noted in the optical microscopy and SEM studies as a non-birefringent component having an index of refraction slightly lower than that of the dacitic glass and having an "amoeba" texture. Clinoptilolite, cristobalite, plagioclase, and halite were identified by XRD. Well-formed crystals of sodic plagioclase were found coexisting with clinoptilolite in vugs and were considered to be authigenic. In the SEM, these crystals appeared to be thicker than the clinoptilolite, which forms thin platy crystals. EDX analyses indicated differences in the Si/Al ratio and the Na and Ca contents; material removed from the vugs was identified as clinoptilolite and plagioclase by XRD.

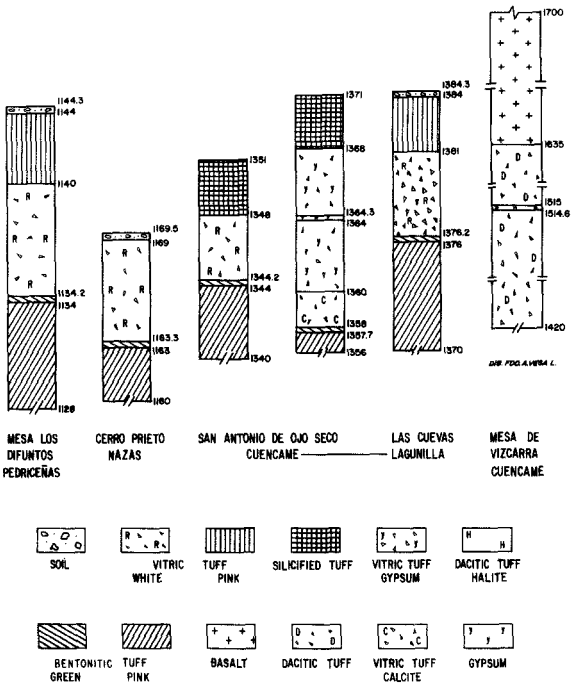

Figure 2. Schematic columnar sections. Altered vitric tuffs overlie bentonitic tuffs, the boundary occurring at 1134.2–1376.2 m elevation. Lower contact of the bentonitic tuff is masked by alluvium. Dacitic vitric tuffs are exposed at elevations >1420 m on southern and western margins of depositional basin. Numbers indicate elevation in meters above sea level.

K-feldspar

K-feldspar occurs as columnar aggregates, which completely replace the parent glass (Figure 3). Optically, it appears as low birefringent aggregates of elongated crystals that are radially oriented towards the interior of the altered glass bubbles or perpendicular to the surface of the shards. SEM shows it as delicate columnar aggregates (Figure 4A) or growths of well-developed crystallites (Figure 4B), which are not associated with any other mineral in the interior of the replaced bubble. Its EDX composition is 64.3% SiO_2, 17.1% Al_2O_3, and 16.4% K_2O (total 97.8%), with the remaining 2.2% being unquantified Na_2O and, possibly, analytical error. This analysis corresponds essentially to pure K-feldspar. The morphology and microtexture of these crystals are different from those of the pyrogenic sanidine phenocrysts (Figure 5) that also occur in the tuff.

https://doi.org/10.1346/CCMN.1990.0380412 Published online by Cambridge University Press

Figure 3. Scanning electron micrograph of altered tuff, showing glass bubbles and shards altered to columnar aggregates of K-feldspar. Sample M3, San Antonio de Ojo Seco, Cuencame. Horizontal bar is 100 μm.

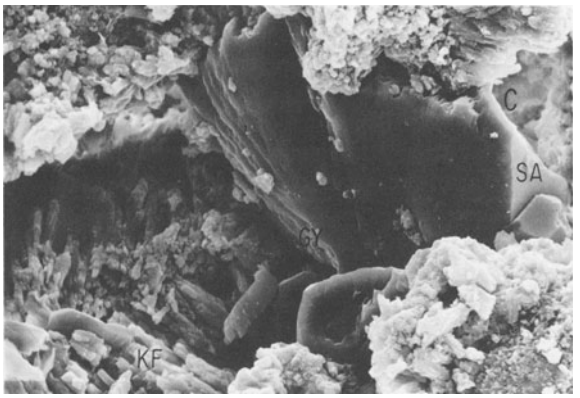

Figure 5. Scanning electron micrograph of altered vitric tuff showing sanidine phenocrysts (SA), K-feldspar altered from glass (KF), chalcedony (C), and gypsum (GY). Sample M10. Horizontal bar is 10 μm.

Chalcedony, cristobalite, quartz

Chalcedony was observed optically as a low-birefringent, massive phase, filling interstices between the altered shards and bubbles. It appears to have been altered to saccharoidal quartz, which increases progressively in concentration towards the silicified tuff at the top of the deposits (Tables 1 and 2). Cristobalite was identified by XRD in the altered vitric tuff and in the bentonitic tuff.

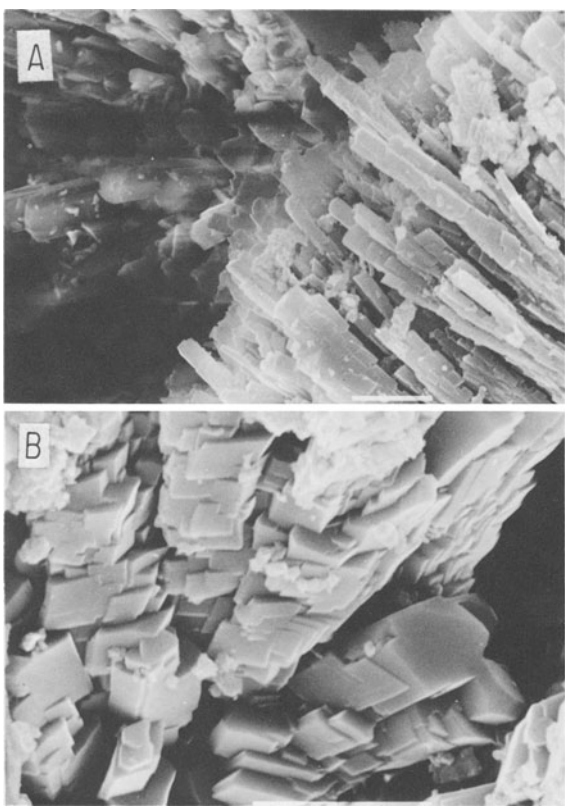

Figure 4. Scanning electron micrographs showing (A) columnar growths and (B) well-developed crystallites of K-feldspar. Columnar growths are oriented radially towards interior of devitrified glass bubble and have completely replaced parent glass. They are not associated with any other mineral phase. Horizontal bar is 10 μm.

Albite

Albite occurs in the altered vitric tuff as a massive authigenic phase, filling interstices. It was best identified by EDX as a SiO_2-, Al_2O_3-, and Na_2O-containing phase, inasmuch as it can easily be mistaken optically for chalcedony and cannot readily be differentiated by XRD from the predominant authigenic K-feldspar or pyrogenic sanidine. The chemical analyses (Table 2) indicate contents of Na_2O averaging 2% (3.1% for sample M3) and <0.8% CaO (0.12% for sample M3), which suggest an albitic plagioclase, because glass was not recognized optically as a major phase in this altered tuff. Albite was identified only in the altered vitric tuff that does not contain clinoptilolite, as indicated by XRD and microscopy.

Montmorillonite

Montmorillonite crystallized as the essential mineral component of the bentonitic tuff as thin, curved, delicate flakes diagenetically produced from the glass (Figures 6A and 6B). EDX analyses indicate that this montmorillonite contains 46.1% SiO_2, 17.9% Al_2O_3, 2.5% K_2O, and 3.2% CaO, which sum to 69.7%; the remaining 30.3% is presumably H_2O and very minor unquantified MgO and Na_2O. It is different from a second montmorillonite, containing Si, Al, no Ca, and minor K, that occurs as a minor authigenic mineral on the prismatic faces of pyrogenic sanidine phenocrysts (Figure 6C).

The more abundant pink montmorillonite and the

https://doi.org/10.1346/CCMN.1990.0380412 Published online by Cambridge University Press

Table 1. Mineralogy of the altered vitric tuff and the bentonitic tuff of the Vizcarra Formation.[1]

Sample	Elevation (m)	Lithology	Mineralogy (wt. %)								
			Q	AL	K-FL	CR	CA	MT	PL	BI	GY
Mesa Los Difuntos, Pedricena											
PE3	1144	atp	30	20	25	25					
PE4	1141	atp	5	15	25	55					
PE6	1138	atw	10	20	10	30	30				
PE2	1134	btg	5	5	5	20		65			
PE1	1132	btp		5	10			85			
Cerro Prieto, Nazas											
TF	1165	atw	45	15	40						
NA22	1163	btg	5	5	5	10	5	70			
NA23	1162	btp	10	5	25	10		50			
NA24	1161	btp	10	5	25	10		50			
San Antonio de Ojo Seco, Cuencame											
CU15	1349	ats	50	10	30				10		
M3	1346	atw	10	10	75					5	
M4	1344	btg	15					85			
M5	1343	btp	10			20		65		5	
M9	1382	ats	50	10	40						
M10	1365	atw	5	10	50			5		5	25
M12	1362	btg	10		5	40		40			5
M14	1359	atw			70		20	10			
M15	1357	btp				20		80			
Las Cuevas, Cuencame											
CU10	1383	ats	40	10	50						
CU11	1380	atw	40	10	50						
CU13	1375	btp	10	5	10	30		50			

[1] Weight percentages estimated from megascopic, optical, X-ray powder diffraction, and scanning electron microscopy data. Q, Quartz; AL, Albite; K-FL, K-feldspar; CR, Cristobalite; CA, Calcite; MT, Montmorillonite; PL, plagioclase; BI, Biotite; GY, Gypsum; atp, altered tuff pink; atw, altered tuff white; ats, altered tuff silicified; btg, bentonitic tuff green; btp, bentonitic tuff pink.

green montmorillonite are dioctahedral, d(006) = 1.504 Å. If the total concentration of exchangeable cations corresponds to the Si/Al tetrahedral substitution, chemical compositions and formulae can be calculated for these montmorillonite materials (Table 6). Various size fractions sedimented from a sodium hexametaphosphate suspension exhibit a basal 001 reflection at 13.2 Å, which upon glycolation expands to 17.6 Å. In K-saturated montmorillonite heated to 300°C, the 001 reflection shifted from 11.9 Å for the unheated material to 15.5 Å after heating, suggesting a low interlamellar charge. The displacement of the basal spacing in Li-montmorillonite, from 15.5 Å (air-dried) to 12.0 Å (heated to 225°C) to 16.5 Å (glycolated), indicates that the site of the charge is in the tetrahedral layer. One-layer (d(001) = 12.28 Å) and two-layer (d(001) = 16.68 Å) spacings were developed for Na-montmorillonite saturated with Li for 2–115 hr, and the intensity of their basal reflection was substantially increased as the Li saturation progressed. Infrared spectroscopy experiments performed on Na-montmorillonite saturated with pyridine, dried, and heated to 150° and 400°C indicate Lewis-type surface activity. This activity is indicated by the persistence of the 1450- and 1620-cm^{-1} vibrations assigned to pyridine joined by the two nitrogen electrons to an empty p-orbital.

The formulae calculated for the green and pink montmorillonite materials indicate comparable degrees of tetrahedral substitution. Mg in excess to that in exchangeable positions was assigned to the octahedral layer. The octahedral layer of the pink montmorillonite has more Al than Mg. From these formulae, the interlayer areas available for cation exchange were calculated to be 119.73 $Å^2$/ion for the green material and 168.27 $Å^2$/ion for the pink material, equivalent to 8.354 and 5.944 esu/cm^2 × 10^{-4}, or 24.23 and 18.66 microcoulombs/cm^2, respectively.

Noncrystalline aluminosilicate material

A noncrystalline aluminosilicate material formed as a dissolution-reprecipitation product from the dacitic glass in the dacitic tuff (Figure 7). It was recognized optically by the absence of birefringence and by a refractive index only slightly less than that of the dacitic glass. Throughout the SEM studies, it was characterized by an "amorphous" or "amoeba-form" microtexture. Its EDX chemical composition is 55.0% SiO_2, 21.3% Al_2O_3, 9.0% CaO, and 1.6% K_2O, total 86.9%.

https://doi.org/10.1346/CCMN.1990.0380412 Published online by Cambridge University Press

Table 2. Chemical composition of the altered vitric tuff and bentonitic tuff of the Vizcarra Formation, Durango.[1]

Sample	Components (wt. %)										
	SiO_2	Al_2O_3	Fe_2O_3	CaO	MgO	Na_2O	K_2O	TiO_2	H_2O^-	H_2O^+	Total
					Mesa Los Difuntos, Pedricena						
PE3	80.00	10.59	1.07	0.84	0.10	2.13	2.75	0.11	0.32	0.76	98.68
PE4	83.40	8.51	0.61	0.66	0	2.10	3.41	0.14	0.54	0.61	99.98
PE6[2]	52.25	6.03	0.96	17.80	1.08	2.13	1.05	0.12	2.35	2.22	99.96
PE2	64.69	12.87	2.91	1.03	2.13	1.70	0.41	0.11	8.70	4.97	99.52
PE1	60.96	14.49	1.49	0.74	5.28	1.62	0.55	0.15	8.77	5.87	99.92
					Cerro Prieto, Nazas						
TF	73.70	13.55	2.30	1.00	0	1.84	5.98	0.29	0.33	0.98	99.97
NA22	51.81	18.61	2.99	9.02	1.68	2.70	1.78	0.62	3.46	5.31	97.98
NA23	55.59	16.98	5.36	2.25	4.07	2.23	1.84	0.82	6.20	4.59	99.93
NA24	56.70	15.74	6.57	1.38	3.38	2.19	2.76	1.08	5.35	4.83	99.98
					San Antonio de Ojo Seco, Cuencame						
CU15	77.38	8.99	1.28	1.82	0	1.46	5.50	0.09	0.42	1.95	98.89
M3	64.60	18.12	1.45	0.12	0	3.10	11.75	0.12	0.29	0.37	99.92
M4	62.55	17.20	1.89	0.73	4.14	2.59	1.11	0.17	3.23	5.44	99.05
M5	74.30	8.49	1.21	0.57	1.62	1.96	0.33	0.10	7.62	3.73	99.93
M9	72.40	14.03	1.94	0.67	0	1.30	7.85	0.17	0.05	0.92	99.33
M10[3]	55.11	12.43	2.05	8.80	0.10	1.55	9.59	0.09	1.82	3.71	98.49
M12	64.89	11.57	1.50	0.55	2.91	1.45	0.31	0.08	11.95	4.01	99.20
M14[4]	61.00	10.14	1.87	7.57	0.18	1.16	7.11	0.14	0.19	3.41	98.80
M15	69.60	10.86	1.45	0.36	3.36	1.78	0.42	0.07	6.65	4.50	99.05
					Las Cuevas, Cuencame						
CU10	65.83	17.90	1.18	0.24	0	1.43	10.48	0.10	0	1.05	98.20
CU11	64.08	17.67	0.43	0.71	0.11	1.74	12.38	0.15	1.58	1.11	99.96
CU13	66.51	14.53	2.01	0.42	2.55	2.13	1.69	0.11	5.00	3.95	98.90

[1] Analyses by X-ray fluorescence, except Na_2O, CO_2, SO_4, and H_2O, by wet chemistry.
[2] Sample also contains 13.97% CO_2.
[3] 3.24% SO_4.
[4] 6.03% CO_2.

The difference from 100% is presumably very minor unquantified Na_2O and some H_2O. Optically, it could hardly be differentiated from the associated glass and was considered as such in the estimation of the mineral content of the dacitic tuff indicated in Table 3.

Clinoptilolite

Clinoptilolite forms well-developed thin plates in the dacitic vitric tuff. It was clearly identified by XRD. In the SEM studies it was differentiated from the coexisting sodic plagioclase by its platy morphology, higher Si/Al ratio, and lower Ca content. The exchangeable cation was not determined. The abundance of clinoptilolite in vugs (Figure 8) or embedded in the glass suggest that it may have crystallized from leached glass or from solution.

Plagioclase

Plagioclase occurs as well-formed crystals (Figure 9) coexisting with clinoptilolite in vugs in the dacitic tuff. Its composition, determined by EDX, indicates a sodic plagioclase containing only minor Ca, different from a more calcic pyrogenic plagioclase that also occurs in the dacitic tuff.

Halite

Halite occurs as cubes (Figure 10) in the dacitic tuff. It was identified by SEM and XRD studies on samples collected south of Cuencame at an elevation of 1515 m.

DIAGENETIC FACIES

Three lithologic units are considered here in the discussion of the diagenetic facies. One, represented by the altered vitric tuff (samples PE3, PE4, PE6, TF, M3, M10, M12, M14, CU10, and CU11 in Tables 1 and 2), is characterized by its pink and white colors. It contains colorless uncollapsed glass bubbles and shards altered to columnar growths of cryptocrystalline K-feldspar (Figures 3 and 4), as well as minor phenocrysts of pyrogenic sanidine, sodic plagioclase, quartz, and biotite; rock fragments; and rare secondary calcite and gypsum. Authigenic albite and chalcedony fill interstices and are progressively altered to saccharoidal and massive quartz in samples collected at higher elevations.

The chemical composition of this altered vitric tuff is best represented by sample M3 (Table 2), which contains 64.60% SiO_2, 18.12% Al_2O_3, 1.45% Fe_2O_3,

https://doi.org/10.1346/CCMN.1990.0380412 Published online by Cambridge University Press

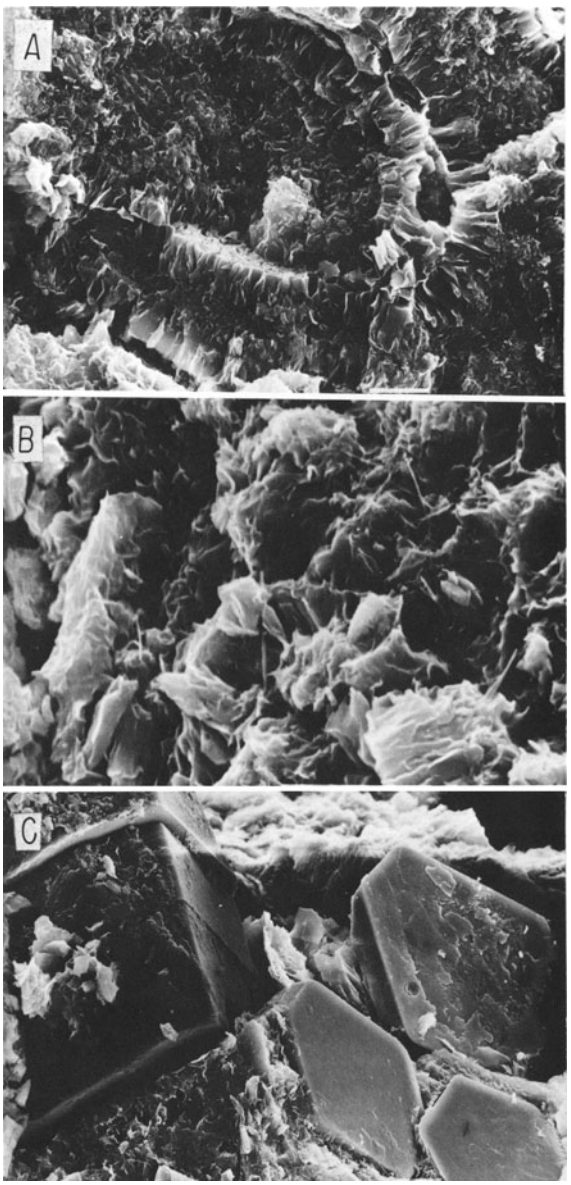

Figure 6. Scanning electron micrographs of the bentonitic tuff showing (A) uncollapsed bubble in which glass has been replaced by montmorillonite; (B), magnified view showing flakes of montmorillonite; (C), sanidine phenocrysts in smectite matrix diagenetically reacted on lateral prisms to non-calcic K-montmorillonite, which is different from the matrix Na-montmorillonite. Sample M5. Horizontal bar is 10 μm.

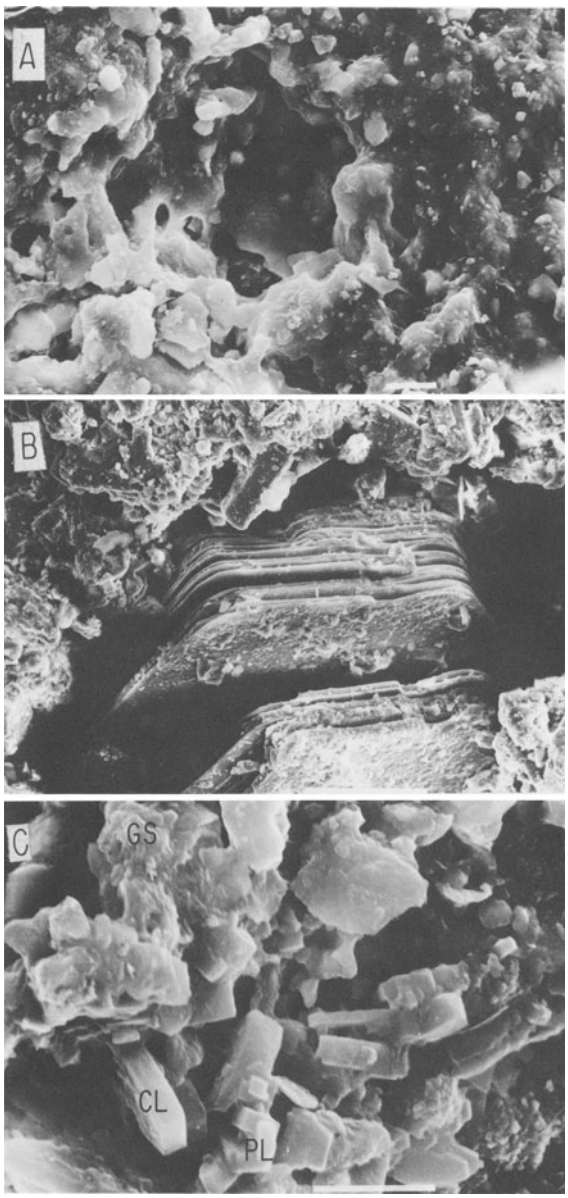

Figure 7. Scanning electron micrographs of dacitic vitric tuff indicating: (A), shapeless and noncrystalline aluminosilicate material developed from dacitic glass; (B), aluminosilicate material cementing glass fragments and biotite phenocryst; (C), clinoptilolite (CL), plagioclase (PL), and glass (GS) partially cemented by the aluminosilicate material. Sample M35. Horizontal bar is 10 μm in 7A and 7C, and 100 μm in 7B.

0.12% CaO, 3.10% Na_2O, 11.75% K_2O, 0.12% TiO_2, 0.29% H_2O^-, and 0.37% H_2O^+, total 99.92%. Other analyses in Table 2 are of similar material that is silicified or that contains secondary calcite or gypsum. Such compositions could indicate a parent glass rich in K_2O. Although high concentrations of K_2O are possible in residual derivative continental magmas (e.g., obsidian) through processes of fractional crystallization (Schairer and Bowen, 1955; Waldbaum and Thompson, 1969; Yund, 1975; Morse, 1970, 1980; Carmichael, 1979; Carmichael *et al.*, 1974), a genesis for this altered vitric tuff associated with magmas of trachytic or phonolitic character can be discarded.

Fresh glass representative of the unaltered pyroclas-

https://doi.org/10.1346/CCMN.1990.0380412 Published online by Cambridge University Press

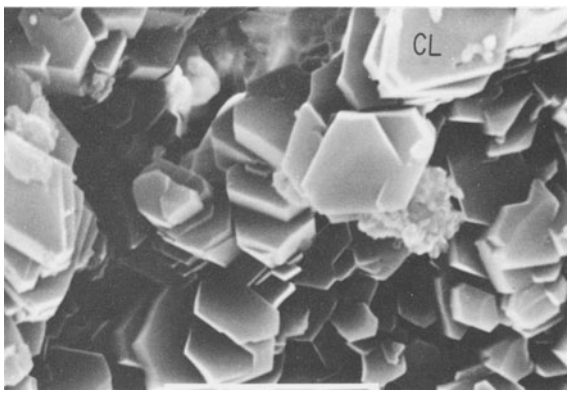

Figure 8. Scanning electron micrograph of clinoptilolite (CL) in vugs in dacitic tuff. Sample M36. Horizontal bar is 10 μm.

tic material could not be found; hence, its characteristics can at best be estimated from those of the altered tuff. The volatile and more soluble components were presumedly lost during the quenching, cooling, and devitrification of the magma (Noble *et al.*, 1967; Noble, 1967, 1970; Nakamura, 1974; Burnham, 1979; Stewart, 1979). The composition of the altered tuff (Table 2) indicates that, from high to low elevations, K_2O/Al_2O_3 decreased and other ratios to Al_2O_3 increased, suggesting a possible pattern of leaching by which Mg, Ca, Fe, and Na were moved downwards. The parent pyroclastic material possibly had a rhyodacitic to alkaline rhyolitic composition, less potassic and more silicic than sample M3 or more potassic and less silicic than sample PE4, which was subsequently modified by a hydration process that removed and replaced components by H^+. The few phenocrysts of sodic plagioclase and quartz, the alteration of glass only to K-feldspar, and the interstitial albite and silica minerals suggest the alteration of a K_2O-rich, MgO- and CaO-poor glass, leaching of some components, crystallization of K-feldspar, and displacement of SiO_2 and

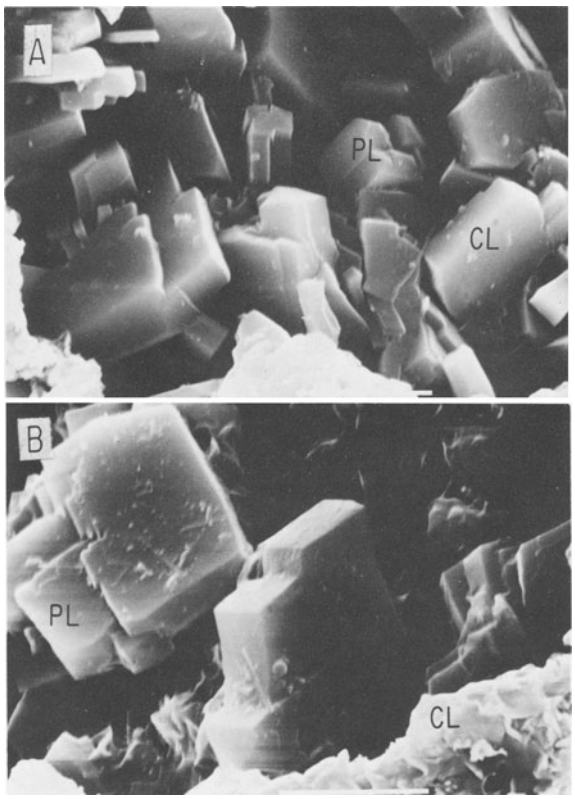

Figure 9. Scanning electron micrographs of plagioclase in dacitic tuff. (A), sodic plagioclase (PL) and clinoptilolite (CL) crystals in vug; (B), sodic plagioclase. Sample M35. Horizontal bar is 10 μm.

Na_2O towards interstitial spaces to form albite and silica minerals.

A second lithologic unit is represented by the bentonitic tuffs which underlie the altered vitric tuff (Figure 2). This facies is characterized by green and pink bentonitic tuffs (samples PE2, PE1, NA22, NA23, NA24, M4, M5, M15, and CU13 in Tables 1 and 2), which

Table 3. Mineralogy of dacitic vitric tuffs of the La Zorra Formation, Durango.[1]

Sample	Elevation (m)	Lithology	Mineralogy (wt. %)									
			GL	PL	CR	CL	Q	HA	MT	BI	AU	OL
M37	1635	b		65	5						20	10
M38	1634	vtd	50		5	45						
M36	1558	vtd	50	5		35	10					
M35	1557	vtd	50	25		10	15					
M33	1553	vtd	50	10		30	10					
M34	1515	vtd	50	20	10	3	5	5	5	2		
C21	1465	vtd	50	25	10	10	5					
C30	1435	vtd	50	25	5	15				5		
C31	1420	vtd	50	20		5	20			5		

[1] Weight percentages estimated from megascopic, optical, X-ray powder diffraction, and scanning electron microscopy studies. b, basalt; vtd, vitric tuff, dacitic; GL, Glass; PL, Plagioclase; CR, Cristobalite; CL, Clinoptilolite; Q, Quartz; HA, Halite; MT, Montmorillonite; BI, Biotite; AU, Augite; OL, Olivine.

https://doi.org/10.1346/CCMN.1990.0380412 Published online by Cambridge University Press

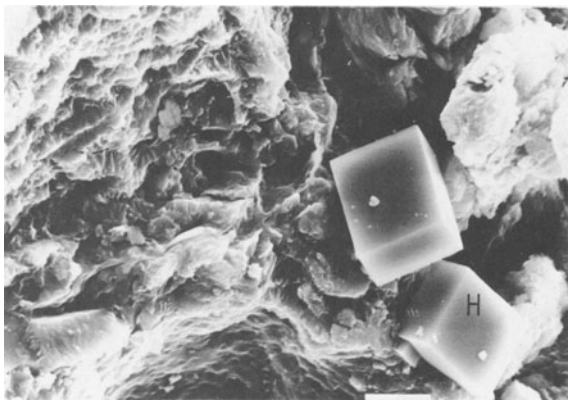

Figure 10. Scanning electron micrograph of halite (H) in dacitic tuff. Sample M34. Horizontal bar is 10 μm.

are very fine grained, plastic, and possess a relict vitroclastic texture. The essential component is montmorillonite (Figure 6), which occurs as thin, curved, delicate crystallites; the montmorillonite coexists with minor phenocrysts of sanidine, sodic plagioclase, quartz, and oxybiotite and rock fragments. The bentonite in contact with the overlying altered tuff is green, 50-cm thick, and has a sanidine and chalcedony content greater than the underlying pink bentonite, which is exposed 4–6 m above a concealed lower contact.

The chemical composition of these bentonitic tuffs is best represented by samples PE1 pink and M4 green (Tables 2 and 5). They contain, respectively, 5.28 and 4.14% MgO and 0.55 and 1.11% K_2O, as opposed to the nil MgO and very high K_2O contents of the overlying altered vitric tuff. The contents of CaO, Na_2O, and SiO_2 are similar. Such compositions suggest a parent vitroclastic material of rhyodacitic composition, possibly deposited in a stagnant lacustrine environment rich in Mg. The hypothesis suggested for the alteration of the overlying altered tuff by descending solutions remains possible, but the very high MgO and the low K_2O and Na_2O contents of the underlying bentonite could suggest that these two lithologic units could represent two different vitroclastic parent materials,

Table 5. Characteristics of the bentonitic tuffs.[1]

Characteristic	Bentonitic tuff	
	PE1 pink	M4 green
Chemical composition (wt. %)		
SiO_2	60.96	62.55
Al_2O_3	14.49	17.20
Fe_2O_3	1.49	1.89
CaO	0.74	0.73
MgO	5.28	4.14
Na_2O	1.62	2.59
K_2O	0.55	1.11
TiO_2	0.15	0.17
H_2O^-	8.77	3.23
H_2O^+	5.87	5.44
Total	99.92	99.05
Cation-exchange capacity (meq/100 g)	65	64
Cation exchange		
Ca^{2+}	20	15
Mg^{2+}	30	20
Na^+	2.7	4.1
K^+	2.6	1.0
Mineralogy (wt. %)		
Montmorillonite	85	85
Quartz	—	15
Sanidine	10	—
Albite	5	—

[1] Chemical composition determined by wet chemistry and X-ray fluorescence. Other characteristics determined by the procedures indicated in the text.

one of which may have been deposited in a stagnant, Mg-rich lacustrine environment.

The third lithologic unit is represented by the dacitic vitric tuff of the La Zorra Formation, which crops out at elevations 1420–1634 m (Figure 2) south and west of Cuencame. This tuff is brown, fine to medium grained, and hypocrystalline. It contains (Table 3) about 50% glass (Figure 7), 3–45% authigenic clinoptilolite (Figures 7C and 8), and 5–25% intermediate to sodic plagioclase (Figure 9) of pyrogenic and authigenic origins; well-crystallized halite occurs at an elevation of 1515 m (Figure 10). An average composition of the dacitic tuff (Table 4) is 65.73% SiO_2, 13.56% Al_2O_3,

Table 4. Chemical composition of dacitic vitric tuffs of the La Zorra Formation, Durango.[1]

Sample	Composition (wt. %)											
	SiO_2	Al_2O_3	Fe_2O_3	CaO	MgO	Na_2O	K_2O	TiO_2	H_2O^-	H_2O^+	Cl	Total
M37	52.13	17.72	7.70	8.67	4.23	3.26	1.23	1.24	1.13	2.13	—	99.44
M38	66.17	13.52	1.32	2.67	1.93	2.16	2.02	0.19	3.46	6.36	—	99.80
M35	66.23	15.62	2.36	2.63	1.61	2.91	2.86	0.47	1.60	3.44	—	99.73
M33	62.54	13.87	2.00	2.29	1.30	1.79	3.20	0.51	3.96	5.47	—	96.93
M34	70.66	13.23	1.71	2.11	0.94	2.15	1.24	0.55	3.81	3.24	0.22	99.86
C21	68.80	13.19	2.41	2.59	1.13	2.10	2.82	0.40	2.78	3.76	—	99.98
C30	68.66	13.08	1.93	3.09	0.81	2.18	2.72	0.36	2.16	4.53	—	99.52
C31	70.12	11.72	2.21	1.85	0.78	2.13	2.54	0.26	1.93	3.08	—	96.62

[1] Chemical analyses by X-ray fluorescence, except Na_2O, Cl, and H_2O by wet chemistry.

https://doi.org/10.1346/CCMN.1990.0380412 Published online by Cambridge University Press

Table 6. Characteristics of the montmorillonite materials.[1]

Characteristic	Montmorillonite PE1 pink	Montmorillonite M4 green
Chemical composition (wt. %)		
SiO_2	53.74	58.08
Al_2O_3	17.96	20.94
CaO	0.92	0.89
MgO	6.54	5.04
Na_2O	2.01	3.15
K_2O	0.68	1.35
H_2O^-	10.86	3.93
H_2O^+	7.27	6.62
Total	99.98	100.00
Cation-exchange capacity (meq/100 g)	65	64
Cation exchange		
Ca^{2+}	20	15
Mg^{2+}	30	20
Na^+	2.7	4.1
K^+	3.6	1.0
Particle size distribution (%)[1]		
97	<12.20 μm	
71	<1.22	
60	<1.04	
48	<0.62	
Structure	dioctahedral	
Charge site	tetrahedral	
Interlamellar charge (esu/cm² × 10^{-4})	8.35	5.94
Interlamellar complexes	one-, two-layer	
Surface acidity	Lewis type	
Interlayer area (Å²/ion)	119.73	168.27
Formula		
PE1: $(Si_{3.88}Al_{0.12})(Al_{1.41}Mg_{0.59})O_{10}(OH)_2(Ca_{0.07}Mg_{0.11}Na_{0.28}K_{0.06})$		
M4: $(Si_{3.86}Al_{0.14})(Al_{1.50}Mg_{0.50})O_{10}(OH)_2(Ca_{0.06}Na_{0.40}K_{0.11})$		

[1] Chemical composition determined by wet chemistry and X-ray fluorescence. Particle size distribution in percentage of particles of diameter less than indicated size in μm. Particle size, structure, charge site, complexes, and surface acidity are the same for both materials.

2.07% Fe_2O_3, 2.49% CaO, 1.38% MgO, 1.61% Na_2O, 2.69% K_2O, 0.41% TiO_2, 3.63% H_2O^-, and 5.39% H_2O^+. Local olivine and augite basalt flows (sample M37, Tables 3 and 4) also occur in this facies.

The diagenetic alteration recognized in this dacitic tuff is different from that found in the two lithologic units described above. In the dacitic tuff, the glass was leached to a noncrystalline aluminosilicate material (Figure 7), which cemented components. Clinoptilolite apparently crystallized from the leached glass (Figures 7 and 9) or from solutions (Figure 8).

Thus, three diagenetic facies have been recognized in the rhyodacitic to rhyolitic tuffs of the Vizcarra Formation and in the dacitic tuffs of the La Zorra Formation in the area of Cuencame-Lagunilla-Pedricena-Rodeo. The younger dacitic pyroclastics of the La Zorra Formation were deposited on high, dry ground and then leached by percolating solutions from which was formed a noncrystalline aluminosilicate phase; clinoptilolite crystallized from leached glass. Halite probably crystallized from saline waters. The rhyodacitic pyroclastics of the Vizcarra Formation which were deposited in lacustrine waters reacted to form high-Mg montmorillonite. The pyroclastics deposited on dry ground overlying the bentonitic tuffs were altered to essential K-feldspar associated with minor albite and silica minerals.

ACKNOWLEDGMENTS

I acknowledge the financial support of the Consejo Nacional de Ciencia y Tecnologia through the grant PCCBBNA-021990. I am also indebted to I. Aguilera, P. Altuzar, P. Giron, A. Lozano, M. Reyes, G. Velazquez, M. L. Chavez, and M. Villegas for their analytical work.

REFERENCES

Burnham, C. W. (1979) The importance of volatile constituents: in *The Evolution of the Igneous Rocks*, H. S. Yoder, ed., Princeton University Press, Princeton, New Jersey, 438–482.

Carmichael, I. S. E. (1979) Glass and glassy rocks: in *The Evolution of the Igneous Rocks*, H. S. Yoder, ed., Princeton University Press, Princeton, New Jersey, 232–234.

Carmichael, I. S. E., Turner, F. J., and Verhoogen, J. (1974) *Igneous Petrology*: McGraw-Hill, New York, 739 pp.

Carrasco, M. (1980) Cartas y Provincias Metalogeneticas del Estado de Durango: Consejo de Recursos Minerales, Mexico, Publ. **22-E**, 63 pp.

Cordoba, D. A. (1960) Estudio Geologico de Reconocimiento de la Region entre Rio Chico y Llano Grande, Municipio de Durango, Edo. de Durango: Thesis. Facultad de Ingenieria, Universidad Nacional A. de Mexico, Mexico City, Mexico, 36 pp.

de Cserna-Gombos, Z. (1956) Tectonica de la Sierra Madre Oriental en Mexico entre Torreon y Monterrey: *XX Congreso Geologico Internacional, Mexico, Monograph*, 87 pp.

de Pablo-Galan, L. (1979) The clay deposits of Mexico: in *Proc. Int. Clay Conf., Oxford, 1978*, M. M. Mortland and V. C. Farmer, eds., Elsevier, Amsterdam, 475–486.

Direccion de Estudios del Territorio Nacional (1978a) Carta Geologica La Lagunilla G13D55, Durango: Secretaria de Programacion y Presupuesto, Mexico.

Direccion de Estudios del Territorio Nacional (1978b) Carta Geologica Cuencame G13D54, Durango: Secretaria de Programacion y Presupuesto, Mexico.

Direccion de Estudios del Territorio Nacional (1978c) Carta Geologica Rodeo G13D42, Durango: Secretaria de Programacion y Presupuesto, Mexico.

Direccion de Estudios del Territorio Nacional (1978b) Carta Geologica Velardena G13D44, Durango: Secretaria de Programacion y Presupuesto, Mexico.

Direccion de Estudios del Territorio Nacional (1978e) Carta Geologica Nazas G13D43, Durango: Secretaria de Programacion y Presupuesto, Mexico.

Enciso, S. (1968) Hoja Cuencame: Instituto de Geologia, Universidad Nacional A. de Mexico, Mexico City, Mexico, map.

Greene-Kelley, R. (1955) Dehydration of the montmorillonite minerals: *Mineral. Mag.* **30**, 604–615.

Jaynes, W. F. and Bigham, J. M. (1986) Multiple cation-

exchange capacity measurements on standard clays using a commercial mechanical extractor: *Clays & Clay Minerals* **34,** 93–98.

Lopez-Ramos, E. (1983) Carta Geologica del Estado de Durango: Instituto de Geologia, Universidad Nacional A. de Mexico, Mexico City, Mexico.

Low, P. R. (1981) The swelling of clay. III. Dissociation of exchangeable cations: *Soil Sci. Soc. Amer. J.* **45,** 1074–1078.

Morse, S. Q. (1970) Alkali feldspars with water at 5 kb pressure: *J. Petrol.* **11,** 221–251.

Morse, S. Q. (1980) *Basalts and Phase Diagrams:* Springer-Verlag, New York, 493 pp.

Nakamura, Y. (1974) The system SiO_2-H_2O-H_2 at 16 kb: *Carnegie Inst. Washington Yearbook* **73,** 259–262.

Noble, D. C. (1967) Sodium, potassium, and ferrous iron contents of some secondarily hydrated natural silicic glasses: *Amer. Mineral.* **52,** 280–286.

Noble, D. C. (1970) Loss of sodium from crystalline comendite welded tuffs in the Miocene Grouse Canyon Member of the Belted Range Tuff, Nevada: *Geol. Soc. Amer. Bull.* **81,** 2677–2688.

Noble, D. C., Smith, V. C., and Peck, L. C. (1967) Loss of halogens from crystallized and glassy silicic volcanic rocks: *Geochim. Cosmochim. Acta* **31,** 215–223.

Occelli, M. L. and Tindwa, R. M. (1983) Physicochemical properties of montmorillonite interlayered with cationic oxyaluminum pillars: *Clays & Clay Minerals* **31,** 22–28.

Perry, E. P. (1983) An infrared study of pyridine adsorbed on acid sites. Characterization of surface acidity: *J. Catal.* **2,** 371–379.

Razo, A. (1960) Estudio Geologico de la Porcion Sur de la Sierra de la Cal y del Prospecto Minero La Preciosa, Mpio. de Nazas, Edo. de Durango: Thesis, Facultad de Ingenieria, Universidad Nacional A. de Mexico, Mexico City, Mexico, 88 pp.

Roldan, J. (1969) Estudio Geologico de Reconocimiento de la region de Penon Blanco, Edo. de Durango: Thesis, Escuela Superior de Ingenieria y Arquitectura, Instituto Politecnico Nacional, Mexico City, Mexico, 61 pp.

Schairer, J. F. and Bowen, N. L. (1955) The system K_2O-Al_2O_3-SiO_2: *Amer. J. Sci.* **253,** 681–746.

Schultz, L. B. (1969) Lithium and potassium adsorption, dehydroxylation temperature, and structural water content of aluminum smectites: *Clays & Clay Minerals* **17,** 115–149.

Sposito, S., Prost, R., and Gaultier, P. (1983) Infrared spectroscopy study of adsorbed water on reduced-charge Na/Li montmorillonites: *Clays & Clay Minerals* **31,** 9–16.

Stewart, D. B. (1979) The formation of siliceous potassic glassy rocks: in *The Evolution of the Igneous Rocks,* H. S. Yoder, ed., Princeton University Press, Princeton, New Jersey, 338–350.

Svoboda, A. R. and Kunze, G. W. (1966) Infrared study of pyridine adsorbed on montmorillonite surfaces: in *Clays and Clay Minerals, Proc. 15th Natl. Conf., Pittsburgh, Pennsylvania, 1965,* S. W. Bailey, ed., Pergamon Press, New York, 277–288.

Waldbaum, D. R. and Thompson, J. B. (1969) Mixing properties of sanidine crystalline solutions. IV. Phase diagrams from equations of state: *Amer. Mineral.* **54,** 1274–1298.

Ward, J. W. (1968) The ratio of adsorption coefficients of pyridine adsorbed on Lewis and Bronsted acid sites: *J. Catal.* **11,** 272–273.

Weaver, C. E. (1958) The effects and geologic significance of potassium "fixation" by expandable clay minerals derived from muscovite, biotite, chlorite, and volcanic material: *Amer. Mineral.* **43,** 839–861.

Wright, A. C., Granquist, W. T., and Kennedy, J. V. (1972) Catalysis by layer lattice silicates. I. The structure and thermal modification of a synthetic ammonium dioctahedral clay: *J. Catal.* **25,** 65–80.

Yund, R. A. (1975) Subsolidus phase relations in the alkali feldspars with emphasis on coherent phases: in *Feldspar Mineralogy,* P. H. Ribbe, ed., Mineralogical Society of America, Reviews in Mineralogy, Vol. 2, Washington, D.C., Y1–Y28.

(Received 8 October 1987; accepted 1 December 1989; Ms. 1718)